Effect of Doping and Annealing Temperatures of Structural Properties of SnO_2 Nanoparticles

Tariq.A.Al-Dhahir and Karrar A. Alsoltani

Department of Physics- College of Education for Pure Science-IbnAl- Haitham, Baghdad University, Iraq

Received : 16 September 2015 ; Accepted : 26 October 2015

Abstract

Nano particles powders of SnO_2 and $Sn_{1-x}Ni_xO_2$ (x = 0.10 and 0.15**)** used in this study are synthesized by sol-gel method. The prepared powders were annealed at 400℃ and 700℃, then characterized their x-ray structure, FTIR and SEM. From, the structural study their grain size by Debye-Scherrer and Williamson-Hall equations, lattice parameters, unit cell volume ,crystal density, internal strain, dislocations density, surface area , and number of unit cells were calculated for different annealing temperatures as well as for doping variations. Single-phase of SnO_2 tetragonal structure is confirmed from a very small variation of structural parameters with annealing temperature. Spherical particles in the nanoscale level, with the size increasing as annealing temperature increase and decrease with doping percentage increase at the same temperature are observed from XRD results. While FTIR study revealed the distortion of the SnO_2 octahedron. Scanning electron microscopy SEM revealed a morphology of fully dense of SnO_2 and that doped samples at 15% which annealed at 400ºC and 700ºC. While energy-dispersive X-ray spectroscopy EDX presented the percentages of Sn, Ni and minor oxygen concentration.

Keywords: Nanoparticles, Crystallinity, Magnetic semiconductor, Distorted octahedron, Clusters, Ionic radius

Effect of Doping and Annealing Temperatures of Structural Properties of SnO_2 Nanoparticles

Tariq.A.Al-Dhahir and Karrar A. Alsoltani

تأثير التشويب ودرجة حرارة التلدين عل الخواص التركيبية لأوكسيد القصدير النانوي SnO_2

طارق عبد الرضا الظاهر كرار امين قدوري السلطاني

كلية التربية للعلوم الصرفة - ابن الهيثم -قسم الفيزياء

الخلاصة

تم تحضير (SnO_2) النانوي النقي والمشوب ($Sn_{1-x}Ni_xO_2$) بحيث (x=0.1 - 0.15) المستخدمة في هذه الدراسة بطريقة الصول – جل .تم تلدين المساحيق المحضرة عند درجة حرارة (400℃) و(700℃)، بعدها تم تشخيص المساحيق باستخدام (XRD، FTIR, SEM). من دراسة الخواص التركيبية تم حساب الحجم الحبيبي بطريقة ديباي – شرر وبطريقة وليامسون – هول وثوابت الشبيكة والحجم البلوري والكثافة البلورية والمطاوعة المجهرية وكثافة الانخلاعات والمساحة السطحية النوعية وعدد خلايا الوحدة ولدرجات تلدين ونسب تشويب مختلفة.تبين ان أوكسيد القصدير النقي والمشوب احادي الطور وهو الطور الرباعي مع تغير قليل في ثوابت الشبيكة ويحتوي على جسيمات كروية الشكل في البنية النانوية ، و كذلك تبين من نتائج حيود الشعاع السيني ان زيادة درجة حرارة التلدين تؤدي الى زيادة الحجم الحبيبي ، بينما ينقص الحجم الحبيبي عند زيادة نسبة التشويب عند نفس حرارة التلدين.ومن دراسة أطياف الاشعة تحت الحمراء (FTIR) للمساحيق تبين تشوه الشكل الثماني لأوكسيد القصدير، ومن خلال المجهر الالكتروني الماسح (SEM) ظهر المسحوق النانوي لأوكسيد القصديرالنقي بشكل تكتل بالإضافة الى العينات المشوبة بالنيكل عند درجة حرارة تلدين (400℃) و(700℃)، اما كاشف الاشعة السينية المشتت للطاقة (EDX) فيبين نسب العناصر الموجودة وهي القصدير والنيكل وجزء قليل من الاوكسجين.

الكلمات المفتاحية : الجسيمات النانوية ، التبلور ، شبه الموصل المغناطيسي ، تشوه الجسيم الثماني ، التجمعات الحبيبية ، نصف القطر الايوني

Introduction

Materials with nanoscale dimensions drew the attention of scientists and researchers because of their important properties, which distinguish it from other normal materials [1].Tin dioxide, SnO_2 is an n-type semiconductor of wide energy gap (E_g= 3.6eV, 300 K) normally known as cassiterite, with rutile of tetragonal structure of space group ($P4_2/mnm$) and lattice parameters,

a=4.74 Å and c=3.19Å [2]. Due to its known optical, electrical and other properties SnO_2 used in a wide range of applications such as, solar cell, solid-state gas sensors, transparent conducting electrodes, rechargeable Li batteries and optical electronic devices [3].

Since it has a potential application, many processes developed to synthesize the nanostructure of SnO_2, likes spray pyrolysis [4], hydrothermal methods [5,6], evaporating tin grains in air [7], chemical vapor deposition [8], thermal evaporation of oxide powder [9], rapid oxidation of elemental tin [10], and sol-gel method [11]. SnO_2 has been single doped with each of In, Ti, As, Sb elements in order to modify its properties. Recently, SnO_2 doped with 3d-transition metals has displayed a converting of nonmagnetic semiconductor into a magnetic semiconductor. Therefore, dilute magnetic semiconductors (DMS) is occurred and followed by the achievement of the presence of ferromagnetism at room temperature or above room temperature in various oxide semiconductors, the exhibition of ferromagnetism along with other properties SnO_2 revealed applications in magnetic optoelectronic devices.

Kuppan et al [12] found ferromagnetism in all Ni doped SnO_2 powder samples at room temperature and their Ni doped samples exhibited highest saturation magnetic moment of 0.573memu/g at a Ni doping level of 10 at.%.

According to our knowledge, most of work has been reported on synthesize of Ni doped nanoparticle SnO_2 semiconductor, and not match work about the structure. Therefore, XRD, FT-IR, SEM, and EDX of the prepared powder samples attempt here to synthesis Ni doped SnO_2 powders by sol-gel and to study the influence of different Ni doping level its structure.

Experimental work

Synthesis

Sol-gel method is used to prepare pure SnO_2 by dissolving 3.5g of Tin (IV) chloride penthydrate (Promchimperm Co,98%,$SnCl_4.5H_2O$)in 100ml of ethanol (Scharlab S.L,99.9%) under vigorous stirring 4ml of ammonia was added to the above solution drop by drop under stirring. When the reaction completed, an opal gels were filtered and washed with ethanol to

remove impurities The obtained powder of tin oxide was annealed at 400℃ .While the Ni doped SnO_2 is performed by using the basic precursors for the preparation of $Sn_{1-x}Ni_xO_2$ (where x = 0.10, 0.15), in which $SnCl_4.5H_2O$ and $Ni(NO_3)_2.6H_2O$ (Riedel-DE Haen AG, 99.98%) are the starting materials followed by the same procedure as for undoped SnO_2. Finally the obtained powders Ni:SnO_2 were annealed at 400℃ and 700℃.

Characterization

The obtained powders were carefully subject to the following characterization studies. Powder XRD pattern was recorded by using SHIMADZU model Japan (6000) diffractometer within the 2θ range of 20 to 80° with Cu-k_α radiation of wavelength (λ= 1.5406Å) . The filament current and operating voltage were kept at 30mA and 40KV respectively. Infrared spectra were measured by using a FTIR-600 spectrometer biotech WQF-520 model a PC with software analysis. Spectra were recorded at a resolution 4 cm^{-1} and scans times 10 recorded between 400 and 1800 cm^{-1}. Scanning Electrons microscope type (Inspect S 50) and (EDX) (Energy Dispersive X-Ray Detection) are used.

Results and Discussion

XRD measurements

Figure 1 shows the X-ray diffraction patterns of prepared pure and Ni doped SnO_2 powder samples of different doping in different air-annealed temperatures .Fig.1a present XRD pattern of the pure SnO_2 annealed at 400℃ and the doped $Sn_{1-x}Ni_xO_2$ (x=0.1)which are annealed at 400℃ and 700℃. In which the diffracted peaks of pure SnO_2 annealed at 400℃ agrees very well with tetragonal structure of SnO_2 (JCPDS card no. 41-1445) and with lattice constant a=4.7461Å and c= 3.2106 Å, while for doped one at 400℃ revealed peaks the same as for pure except a decrease in peaks intensity, no measurable changes in 2 theta and the peaks become wider due to their small particle size and no indication for nickel or nickel oxides. The same behaviors for the same compound showed by Ahmad et al [13], but in the different doping (0.01, 0.03, 0.05, 0.07 and 0.09) and different annealing temperatures. They attributed it to the degradation the degree of crystallinity, which arises from the crystal defects

around the dopants and the charge imbalance arising from this defect will change the stoichiometry of the materials. To investigate the presences of Ni and the change in degree of crystallinity, the sample is annealed at 700℃ for 2h. The XRD patterns of it presented in Fig.1A.(Its include a pure SnO_2 and other peaks of NiO (JCPDS card no. 04-0835), as well as their crystallinity increases according to peak intensity increases of the sample and the FWHM decreases for this in annealing temperature . Due to observation of an additional peak, some appreciable change in peak positions taken place, which is resulted in the little change in lattice constants of the annealed sample at 700℃. The variations in the lattice constant due to the ionic radius of Ni^{+2} is 69pm where as that of Sn^{+4} is 71pm.The Ni ion substitutes the Sn^{+4} ions in the crystal due to comparable ionic radius. However, the decrease in the lattice parameter may be due to the smaller ionic radius of Ni ions.

XRD patterns for the sample doped by 15% are present in Fig.1B. It shows the same behavior for 10% doped one. At 400℃ very small changes is appear in the intensity and FWHM of the peaks. This resulted from the change in the degree of crystallinity. For 700℃ the intensity of SnO_2 peaks as well as the appearance of NiO peaks are increased. Therefore, the degree of crystallinity is increased and decreased in the lattice constant were taken place. This is due to dopant increase as well as the increase in the annealing temperature. The Rietveld refinement of the X-ray diffraction data has been done by using fullprof software [14] for pure and Ni doping SnO_2.

Effect of Doping and Annealing Temperatures of Structural Properties of SnO_2 Nanoparticles

Tariq.A.Al-Dhahir and Karrar A. Alsoltani

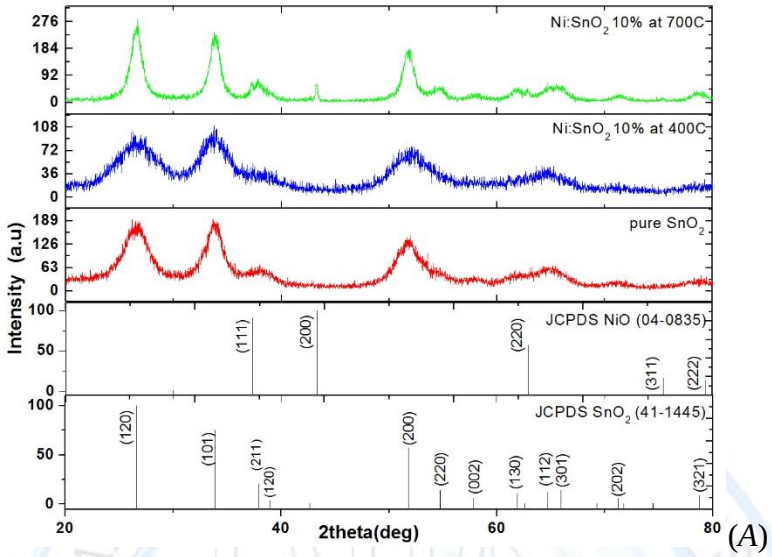

(*A*)

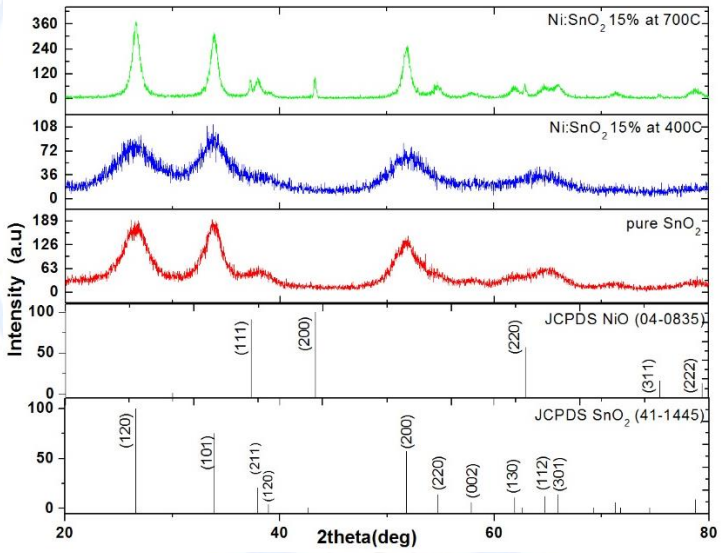

(*B*)

Figure 1: X-ray diffraction patterns of Pure SnO_2, NiO, and Ni doped SnO_2 of prepared samples. (A)Include 10% dopant annealed at 400℃ and 700℃ (B) Include 15% dopant annealed at 400℃ and 700℃

For the tetragonal structure, lattice parameters can be calculated from :

$$1/d_{hkl}^2 = h^2 + k^2/a^2 + l^2/c^2$$

Where h, k, and l are all integers, (hkl) is the lattice plane index, and a and c are lattice constants. The crystallite size of undoped and Ni doped SnO_2 powder samples for all the dopant levels was calculated using Debye-Scherrer formula [15]:

$$D = k\lambda/\beta \cos\theta$$

Where k is a constant, λ is the diffraction wavelength of Cu Kα (λ = 1.5406 Å), β is the full width at half maximum (FWHM), and θ is the diffracted angle, respectively. In addition, by using Williamson-Hall to calculate crystallite size and strain [16]:

$$\beta \cos\theta = (k\lambda/D) + 4\varepsilon \sin\theta$$

Where ε represented the internal strain ,D crystallite size (nm), λ wavelength of x-ray, k constant equals to 0.9,β is the full width at half maximum (FWHM), and θ is the diffracted angle the grain size of particles calculated according to Williamson-Hall different from Debye-Scherrer due to the internal strain. From XRD we can calculate x-ray density of powder by using this equation [17]:

$$\rho_{X\text{-}ray} = Z\ M_{wt}/V\ N_a$$

Where ρ: density (g/cm^3), M_{wt}: molar mass (g/mol), Z: the number of atoms: unit cell size (cm^3), and N_a: Avogadro number (1/mol)

The specific surface area can be calculated by following equation [18]:

$$S.S.A = 6*10^3/D\rho_{X\text{-}ray}$$

And we can find dislocation density (δ) and number of unit cells (n) is calculated using the relation [19,20]:

$$\delta = 1/D^2$$

$$n = \pi D^3 /6\ V$$

Their calculated values will be presented in table 1.

Table (1): shows grain size by Debye-Scherrer equation and W-H, lattice parameter, X-ray and dislocations density, Specific surface area, and number of unit cells

Sample	Pure SnO_2	400℃		700℃	
		10% Ni-SnO_2	Ni-SnO_2 15%	10% Ni-SnO_2	Ni-SnO_2 15%
D_{D-S} (nm)	3.62	2.3	2.186	6.5	6.36
D_{W-H} (nm)	3.84	2.5	2.37	6.67	6.7
ε	-0.00623	-0.00121	0.0043	-0.00308	-0.00115
a=b (Å)	4.7461	4.8004	4.7404	4.7384	4.7367
c (Å)	3.2106	3.2055	3.1937	3.1800	3.1830
V(Å^3)	72.3202	73.86703	71.76689	71.39874	71.41483
ρ_{X-ray}(g/cm^3)	6.92	6.506	6.5577	6.73113	6.5901
SS.A (m^2/g)	239.518	400.968	418.553	137.136	143.154
δ(1/m^2)	$7.63*10^{16}$	$1.89*10^{17}$	$2.09*10^{17}$	$2.36*10^{16}$	$2.47*10^{16}$
n	343.2768	86.20079	76.17365	2012.927	1885.217

Fourier transforms infrared (FTIR):

Tin dioxide has a tetragonal rutile crystalline structure with point group D_{4h} according to Schoenflies notation and space group $P4_2/mnm$ according to international notation. The unit cell consists of two formula per unit cell; it contents six atoms, two Sn atoms (One in the center and the other at corner of the unit cell) and four oxygen atoms. An approximate octahedron is formed from the site of metal and oxygen atoms [21]. Each Sn atom is situated

amidst six oxygen atoms, which approximately form the corners of a regular octahedron. In which oxygen atoms are surrounded by three tin atoms, which form the corners of an equilateral triangle. The lattice parameters are a=b=4.7461Å, and c=3.2106Å. The ionic radii for O^{-2} and Sn^{+4} are 71pm and 69 pm, respectively. The 6 atoms in the unit cell give a total of 18 branches for the vibrational modes in the first Brillouin zone

$$\Gamma=A_{1g}+ A_{2g} +B_{1g}+ B_{2g} +E_g +2A_{2u} +B_{1u}+B_{2u}+ 4E_u$$

Two of them are IR active mode, which are A_{2u} single mode and E_u triply degenerated are active only in IR because these modes involve a change in the dipole moment.

Fig 2(A) shows FTIR spectrum for pure SnO_2 with the peak positions at 542, 590, and 677cm^{-1}, which are assigned as a fingerprint of SnO_2 .A band centered at 590 cm^{-1} is attributed to A_{2u} and assigned to the Sn-O stretching vibration. The peaks around 542 cm^{-1} and 677cm^{-1} are for triply degenerated which are assigned to the asymmetric Sn–O–Sn stretching mode of the surface-bridging oxide which appeared as an absorptions peaks in that range (Patil et al 2003 [22]. The spectra changes can be easily attributed to changes in size and shape of the SnO_2 particles (Gu et al 2003) [23].

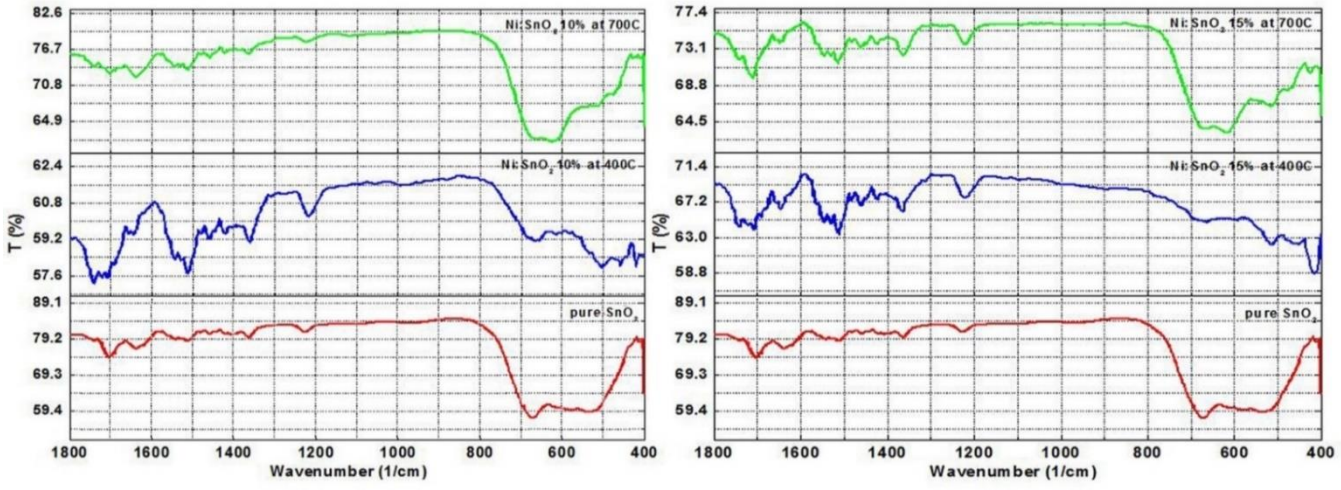

(A) *(B)*

Effect of Doping and Annealing Temperatures of Structural Properties of SnO_2 Nanoparticles

Tariq.A.Al-Dhahir and Karrar A. Alsoltani

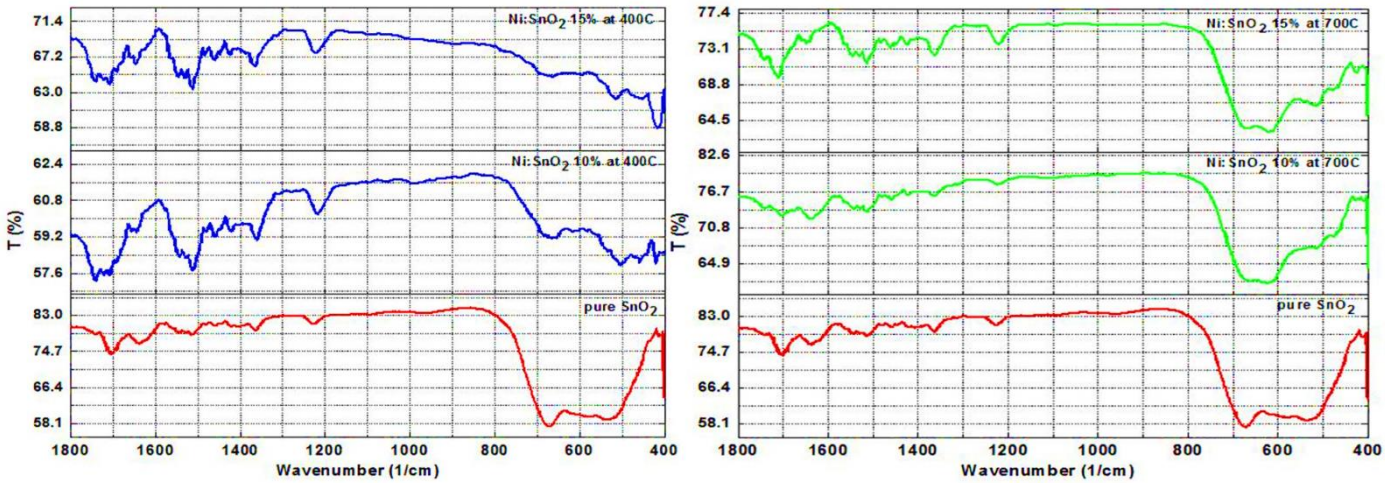

(C) *(D)*

Figure 2: FT-IR spectra of Pure SnO_2 and doped $Sn_{1-x}Ni_xO_2$ nanoparticles (A) Include 10% at 400℃ and 700℃ (B) Include 15% at 400℃ and 700℃ (C) Include 10% and 15% at 400℃ (D) Include 10% and 15% at 700℃

3.3 Effect of annealing and doping on FTIR

Fig 2(A) also involved Ni-SnO_2 10% which are annealed at 400℃ and 700℃. The spectrum at 400℃ revealed peaks at 428, 471, 509, and 663cm^{-1}. It is noted that the number of peaks increases, broadens and decreases in intensity with doping percentage increase. This can be attributed to the reduction of particle size with doping. Secondly, the broadening can also be attributed to the defects generated in the system. The peaks at 428 and 471cm^{-1} belong to NiO transverse optical mode [24]. The broad absorption band in the region of 600-700 cm^{-1} is assigned to Ni–O stretching vibration mode; the broadness of the absorption band indicates that the NiO powders are nanocrystals. While the triply degenerated peaks 663 and 509 cm^{-1} peaks of SnO_2 are shifted to lower wave number. The spectrum at 700℃ revealed peaks at 428, 474, 519, 617 and 663cm^{-1} at 700℃ are presented in figure 2(A).The doping in turns

distorted the octahedron of SnO_2, then resulted in shifting the peaks to lower wavenumber of the modes. According to doping, the bond lengths of $Sn_{1-x}Ni_xO_2$ are changed from those of NiO_2 and SnO_2, and allow the oxygen position change and octahedral distortion to take place in the unit cell. The oxygen positional is decreased when the Ni cation (which has a smaller ionic radius) was substituted the Sn cation. As a result, the octahedral is distorted, in order to keep the central atom in the octahedron can retain a constant position. From FTIR spectra of the samples are clear that there are changes in the shapes and positions of IR peaks indicating that Ni might have been incorporated in SnO_2 host. The bands exhibited in the low wavenumber region of 428-663cm^{-1} might be due to vibration of antisymmetric Sn-O-Sn mode of tin oxide. The most important IR feature is the peak at 565.2 cm^{-1} similar to the surface mode of IR peak at 564 cm^{-1} in the SnO_2 nano powders resulting from the nano size effect.

Fig 2(B) also involved Ni-SnO_2 15% which are annealed at 400℃ and 700℃. The spectrum at 400℃ revealed a new absorption band at 667,515,451 and 420 cm^{-1}, which behave the same as that for Ni-SnO_2 10%, but a little bit stronger than it. While that heated to 700 C revealed the peaks at 671,617, 5l9, 490 and 424 cm^{-1} with a very strong and broad band at 671 cm^{-1}. Intensity increases this due to the crystallinity increases as it is shown from the xrd of the sample fig.1(B).

Fig.2(C) presented the increase of doping at 400℃, in which for 10% of the peaks 663,509,471 and 428cm^{-1} .while for 15% ,667 ,515,451 and 420cm^{-1}. It is clear from presented peaks wave number is shifted, The O-Sn-O stretching vibration increases by 4cm^{-1} and the 509 to 6 cm^{-1} , and the 471 and 428 cm^{-1} are shifted to lower wave number at 451 and 420cm^{-1} this due to grain size that the all the vibrations broadens with the increase in doping. This can be attributed to the reduction of particle size with doping. Secondly, the broadening can also be attributed to the defects generated in the system with 141pm

Fig.2(D) presented the increase of doping at 700℃, in which for 10% the peaks 663,,617,519,474, and 428 cm^{-1} .while for 15% ,671,617,519,490 and 424cm^{-1}. It is clear

from presented peaks wave number shifted, due to change in the O-Sn-O stretching vibration and that is this due to grain size decrease.

3.4 Scanning electron microscope (SEM) and (EDX) :

SEM and EDX of the samples are presented in Figure 3, show the typical SEM morphology of synthesis SnO_2 samples pure and doped which are annealed at 400℃ and 700℃. EDX give an idea of the chemical composition and map distribution of the elements on the surfaces. Fig 3(A) depicts the morphology of the pure SnO_2 nano powder, which are, annealed at 400℃ and its EDX spectra analysis shows the synthesized products, which consists of Sn and a minor oxygen concentration. Fig 3(B) for 15% Ni doping SnO_2 sample at 400℃, its SEM image shows the presence of aggregates of small nanoparticles and the presence of Ni is confirmed from EDX analysis. This supports the XRD results for the same sample. Fig 3(C) for 15% Ni doping SnO_2 sample at 700℃. Depicts the formation of grain boundaries in the Ni-doped SnO_2. It may be due to the increase in density and of the grain size as temperature increases from 400 to 700℃. The EDX show the presence of Ni. SEM for all sample shows spherical structures are formed along with agglomerated clusters of particles.

Effect of Doping and Annealing Temperatures of Structural Properties of SnO_2 Nanoparticles

Tariq.A.Al-Dhahir and Karrar A. Alsoltani

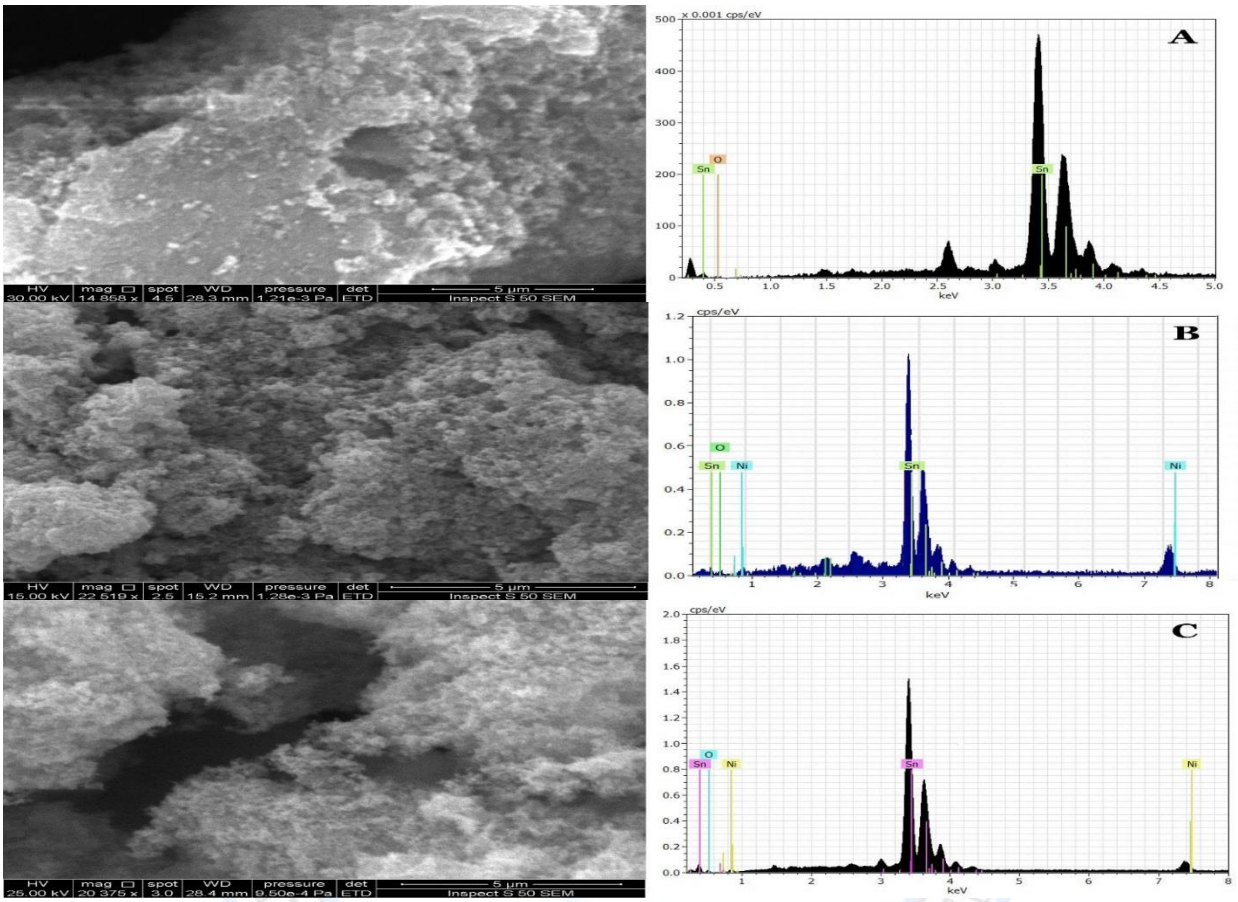

***Figure* 3: show SEM and EDX of tin dioxide (A) pure, (B) 15% doping at 400℃ and (C) 15% doped at 700℃**

Conclusions

Pure and doped nano crystalline SnO_2 powder were successfully synthesized via a simple sol-gel. The size of particles can be tuned from 2.2 to 7nm at different doping and heating at different temperatures. SnO_2 nanopowder with tetragonal structure is observed for as prepared and doped as well as for annealing at 400℃ and 700℃. FTIR spectra shows, that doping resulted a change in peak numbers and shifted in their wave number. SEM Show a dense of agglomerated clusters and EDX shows the presence of Sn and O as well as the doped Ni.

References

1. Raghumani Singh Ningthoujam, S.K. Kulshreshtha, "Nanocrystalline SnO_2 from thermal decomposition of tin citrate crystal: Luminescence and Raman studies" .,Materials Research Bulletin. , 44, pp. 57-62, (2009).
2. ThanhBinh Nguyen, ThiThanhBinh Le and Ngoc Long Nguyen , "The preparation of SnO_2 and SnO_2:Sb nanopowders by a hydrothermal method" Adv. Nat. Sci.: Nanosci. Nanotechnol., 2(1), pp.1-4, (2010),
3. Suresh Sagadevan, " Preparation, Structural and Electrical Properties of Tin Oxide Nanoparticles" J NanomaterMolNanotechnol., 1000157 (4),pp.1-4,(2015).
4. F Paraguay-Delgado, W. Antunez-Flores, M. Miki-Yoshida, A. Aguilar-Elguezabal, P.Santiago, R. Diaz, J.A. Ascencio," Structural analysis and growing mechanisms for long SnO_2 nanorods synthesized by spray pyrolysis"Nanotechnology 6 (16),pp.0957-4484, (2005).
5. B. Cheng, J.M. Russell, W. Shi, L. Zhang, E. T. Samulski," Large-Scale, solution-phase growth of single-crystalline SnO_2 nanorods" J. Am. Chem. Soc. , 126 (19), pp.5972–5973,(2004).
6. S. Fujihara, T. Maeda, H. Ohgi, E. Hosono, H. Imai, S. Kim," Hydrothermal routes to prepare nanocrystalline mesoporous SnO2 having high thermal stability"Langmuir,20(15),pp. 6476–6481 ,(2004).
7. J. Duan, S. Yang, H. Liu, J. Gong, H. Huang, X. Zhao, R. Zhang, Y. Du," Single Crystal SnO2 Zigzag Nanobelts" J. Am. Chem. Soc, 127 (17), pp.6180–6181 ,(2004).
8. Y. Liu, E. Koep, M. Liu,,A Highly Sensitive and Fast-Responding SnO_2 Sensor Fabricated by Combustion Chemical Vapor Deposition" Chem. Mater. 17, pp.3997-4000 , (2005).
9. Z.R. Dai, J.L. Gole, J.D. Stout, Z.L. Wang," Tin Oxide Nanowires, Nanoribbons, and Nanotubes" J. Phys. Chem. B 106,pp.1274-1279, (2002).

10. J.Q. Hu, X.L. Ma, N.G. Shang, Z.Y. Xie, N.B.Wong, C.S. Lee, S.T. Lee." Large-Scale Rapid Oxidation Synthesis of SnO_2 Nanoribbons"J. Phys. Chem. B ,106 (15), pp.3823–3826. , (2002).

11. F. Pourfayaz, A. Khodadadi, Y. Mortazavi,S.S. Mohajerzadeh," CeO2 doped SnO2 sensor selective to ethanol in presence of CO, LPG and CH 4" j.Sensors and Actuators B,1(108),pp.172-176,(2005).

12. M. Kuppan, S. Kaleemulla, N.Madhusudhana Rao, N. Sai Krishna, M. RiganaBegam, andM. Shobana ," Structural and Magnetic Properties of Ni Doped SnO_2", Advances in Condensed Matter Physics , Article ID 284237, pp. 1-5,(2014).

13. Arham S.Ahmed, Shafeeq M.Muhameda, M.L.Singla, SartajTabassum, Alim H.Naqvi, AmeerAzam, "Band gap narrowing and fluorescence properties of nickel doped SnO_2 nanoparticles". Journal of Luminescence ,131 ,pp. 1–6., (2011).

14. Young, R. A. ;Introduction to the Rietveld method," The Rietveld Method, edited by R. A. Young ,Oxford University Press, Oxford",pp.1–38., (2011).

15. Fang LM, Zu XT, Li ZJ, Zhuc S, Liu CM, ZhoueWL,Wang LM "Synthesis and Characteristics of Fe3+-doped SnO_2 Nanoparticles via Sol–Gel Calcination or Sol–Gel-Hydrothermal Route", J. Alloys Comp., 454, pp.261–267,(2008), ,

16. Yendrapati Taraka Prabhu, KalagaddaVenkateswara Rao, VemulaSesha Sai Kumar, Bandla Siva Kumari," X-Ray Analysis by Williamson-Hall and Size-Strain Plot Methods of ZnO Nanoparticles with Fuel Variation "World Journal of Nano Science and Engineering, 1(4),pp. 21-28, (2014) .

17. Stella KC, Nesaraj AS."Low temperature soft chemical synthesis of bright blue CoAl2O4 spinel particles. J.Nepal Chem. Soc.; 25,pp. 62-69.(2010).

18. Jiji A, Joseph N, Donald RB, Daniel M, Amit S, You Qiang," Size-Dependent Specific Surface Area of Nanoporous Film Assembled by Core-Shell Iron Nanoclusters", J. Nanomater., 54961, pp. 1-4(2006),.

19. A. Gaber, M. A. Abdel- Rahim, A. Y. Abdel-Latief, Mahmoud. N. Abdel-Salam, " Influence of Calcination Temperature on the Structure and Porosity of Nanocrystalline

SnO_2 Synthesized by a Conventional Precipitation method" J. Electrochem. Sci., 9,pp. 81 – 95,(2014).

20. Sing P, Kumar A, Kaushal A, Kaur D, Pandey A, Goyal RN, "In situ high temperature XRD studies of ZnO nanopowder prepared via cost effective ultrasonic mist chemical vapour deposition". Bull.Mater.Sci.31(3), pp. 573-577(2008).

21. Decius J.C and Hexter R.M;Molecular Vibrations in Crystal .MicGraw –Hill Inc . ;(1977)

22. Patil P S, Kawar R K, Seth T, Amalnerkar D P and Chigare P S ," Effect of substrate temperature on structural, electrical and optical properties of sprayed tin oxide (SnO_2) thin films"j Ceram. Int. 7(29) , pp. 725–734,(2003).

23. Gu F, Wang S F, Lu M K, Qi Y X, Zhou G J, Xu D and Yuan D R," Luminescent properties of Mn^{2+}-doped SnO_2 nanoparticles" Inorg. Chem. Commun., 6 , pp. 882–885(2003).

24. M. Kanthimathi, A. Dhathathreyan, B.V. Nair,"Nanosized nickel oxide using bovine serum albumin as template", Mater. Lett., 58 ,pp. 2914–2917(2004).